

Control of passivation and compensation in Mg-doped GaN by defect quasi Fermi level control

Cite as: J. Appl. Phys. **127**, 045702 (2020); <https://doi.org/10.1063/1.5126004>

Submitted: 28 August 2019 . Accepted: 05 January 2020 . Published Online: 22 January 2020

A. Klump , M. P. Hoffmann, F. Kaess , J. Tweedie, P. Reddy , R. Kirste, Z. Sitar , and R. Collazo



[View Online](#)



[Export Citation](#)



[CrossMark](#)

ARTICLES YOU MAY BE INTERESTED IN

Monolayer GaN excitonic deep ultraviolet light emitting diodes

Applied Physics Letters **116**, 013101 (2020); <https://doi.org/10.1063/1.5124828>

Pinning of energy transitions of defects, complexes, and surface states in AlGaN alloys

Applied Physics Letters **116**, 032102 (2020); <https://doi.org/10.1063/1.5140995>

Nanoscale electro-thermal interactions in AlGaN/GaN high electron mobility transistors

Journal of Applied Physics **127**, 044502 (2020); <https://doi.org/10.1063/1.5123726>

[SUBMIT TODAY!](#)

Journal of
Applied Physics

SPECIAL TOPIC:
Antiferromagnetic Spintronics

Control of passivation and compensation in Mg-doped GaN by defect quasi Fermi level control

Cite as: J. Appl. Phys. **127**, 045702 (2020); doi: [10.1063/1.5126004](https://doi.org/10.1063/1.5126004)

Submitted: 28 August 2019 · Accepted: 5 January 2020 ·

Published Online: 22 January 2020



View Online



Export Citation



CrossMark

A. Klump,^{1,a} M. P. Hoffmann,¹ F. Kaess,¹ J. Tweedie,² P. Reddy,² R. Kirste,² Z. Sitar,^{1,2} and R. Collazo¹

AFFILIATIONS

¹ Department of Materials Science and Engineering, North Carolina State University, Raleigh, North Carolina 27695-7919, USA

² Adroit Materials, Inc., 2054 Kildaire Farm Rd., Cary, North Carolina 27518, USA

^aAuthor to whom correspondence should be addressed: ajklump@ncsu.edu

ABSTRACT

A defect quasi Fermi level (dQFL) control process based on above bandgap illumination was applied to control H and V_N -complexes, which are the main contributors to the passivation and self-compensation, respectively, in Mg:GaN grown via metalorganic chemical vapor deposition. Secondary ion mass spectrometry measurements confirmed that the total Mg incorporation was unaffected by the process. However, the total H concentration was reduced to similar levels obtained by post-growth thermal activation prior to any annealing treatment. Similarly, the 2.8 eV emission in the photoluminescence spectra, attributed to compensating V_N and its complexes, was reduced for the dQFL-process samples. After thermal activation and Ni/Au contact deposition, Hall effect measurements revealed lower resistivities (increased mobilities and free hole concentrations) for dQFL-grown samples with Mg doping concentrations above and below $2 \times 10^{19} \text{ cm}^{-3}$. All these results demonstrate that the dQFL process can effectively reduce the H-passivation and self-compensation of the Mg:GaN films.

Published under license by AIP Publishing. <https://doi.org/10.1063/1.5126004>

I. INTRODUCTION

Achieving p-type conductivity via magnesium (Mg) doping was a major breakthrough in the realization of GaN-based light emitting diodes and laser diodes.^{1,2} However, despite 30 years of research, there are still significant obstacles limiting the electrical properties of Mg:GaN films.^{3,4} First, the electrically active Mg acceptor has a high ionization energy of ~ 170 – 180 meV.⁵ Thus, a significant concentration of Mg atoms in a film remains inactive at room temperature (RT). Second and the focus of this work, are the Mg passivation and self-compensation mechanisms at play when Mg:GaN layers are grown using metalorganic chemical vapor deposition (MOCVD).

MOCVD-grown Mg:GaN films usually exhibit resistivity values greater than $1 \times 10^6 \Omega\text{cm}$. Residual hydrogen, typically present in the MOCVD process, passivates Mg during growth by forming the neutral Mg-H complex⁶ and needs to be activated via post-growth annealing.^{7,8} This post-growth annealing leads to the dissociation of the Mg-H complex and the eventual removal of hydrogen from the crystal. At a Mg doping concentration of around $\sim 2 \times 10^{19} \text{ cm}^{-3}$, the H concentration in the film saturates.⁹ Yet doping with Mg concentrations above $\sim 2 \times 10^{19} \text{ cm}^{-3}$ does not increase the hole concentration. Instead, when the Mg concentration exceeds this

level, the resistivity is increased due to the self-compensation of Mg acceptors. This self-compensation has been attributed to the nitrogen vacancy donor (V_N) and its complexes,^{10–14} such as the Mg- V_N ,¹¹ $V_N\text{-H}$,^{13,14} or $V_{\text{Ga}}(V_N\text{s})$ ($s = 1, 2$, or 3).^{15,16} However, the formation of these complexes is currently not fully understood and no control mechanism exists. All these show that the effects of H-passivation and self-compensation restrict the free hole concentration to the mid- 10^{18} cm^{-3} range at a Mg concentration of $5 \times 10^{19} \text{ cm}^{-3}$ and resistivity values around $0.7 \Omega\text{cm}$.¹⁷

To improve the electrical properties of Mg:GaN layers, it is paramount to eliminate H and V_N -related point defects that incorporate during growth. In this work, we build on our previous work on managing point defect incorporation by adopting a defect quasi Fermi level (dQFL) control process.^{18–22} During growth, the films are illuminated with the above bandgap light that generates a steady-state concentration of electron-hole pairs. The extra minority carriers present in the film mainly shift the quasi-Fermi level for compensating point defects (but not for major dopants). Consequently, the formation energy of the compensating point defects is increased, resulting in their lower concentration in the film.

In this work, we demonstrate the applicability of the dQFL control process in the management of the compensating point defects

in Mg:GaN. Secondary ion mass spectroscopy (SIMS) studies reveal a reduction in H concentration across a range of Mg concentrations when the films are illuminated during growth. Similarly, photoluminescence (PL) spectra demonstrate a reduction in the 2.8 eV emission line attributed to V_N -complexes when the film with Mg concentrations above $2 \times 10^{19} \text{ cm}^{-3}$ was grown under illumination. As a result of the reductions in compensating point defects, electrical measurements revealed significantly lower resistivity for Mg:GaN layers. Therefore, utilizing above bandgap illumination during growth as a dQFL control process is validated as an effective tool in point defect management and undoubtedly effective in improving p-type conductivity for Mg-doped III-nitride films.

II. EXPERIMENTAL DETAILS

GaN films doped with Mg were grown heteroepitaxially on (0001) sapphire using a vertical, cold-walled MOCVD reactor at a pressure of 20 Torr. For GaN layer growth, 67 $\mu\text{mol}/\text{min}$ of triethylgallium (TEG), 0.3 slm of ammonia, and 6.9 slm of N_2 were flown into the reactor; the substrate temperature was held at 1040 °C.²³ Bis-(cyclopentadienyl)magnesium (Cp_2Mg) was used as the Mg precursor with flows ranging from 0.15 to 0.60 $\mu\text{mol}/\text{min}$. A 1.3 μm undoped GaN template was grown on a 20 nm low temperature (650 °C) AlN nucleation layer, providing for a Ga-polar film.²⁴ For SIMS investigations of H in Mg:GaN layers, intercalated 200 nm thick Mg-doped layers with different Mg concentrations separated by 200 nm thick undoped layers were grown on GaN templates. The samples used for electrical resistivity and photoluminescence measurements were 700 nm thick Mg:GaN layers deposited on the GaN template. The Mg doping level ranged from $6 \times 10^{18} \text{ cm}^{-3}$ to $4 \times 10^{19} \text{ cm}^{-3}$. Thermal activation of these samples was done by post-growth annealing in a furnace at 650 °C in a nitrogen atmosphere for 2 h. These activation conditions are used as they provide for sufficient activation to overcome any kinetic limitations at temperatures that are not expected to adversely affect the sample.²⁵

Above bandgap illumination during growth ($E_g \sim 2.9 \text{ eV}$ at 1040 °C) was achieved by using a mercury-xenon arc lamp uniformly irradiating the wafer surface at a power density of $\sim 1 \text{ W/cm}^2$. This excitation power density led to an estimated steady-state carrier concentration of 10^{12} – 10^{14} cm^{-3} , based on the minority carrier lifetime of 10^{-10} – 10^{-9} s ²⁶ and the absorption coefficient of 10^5 – 10^6 cm^{-1} .¹⁸ This excitation power density does not change the majority carrier concentration, but it is sufficient to change the minority carrier concentration that impacts the formation energy of charged point defects such as H, V_N , and complexes. A detailed description of the growth setup with the UV-lamp can be found elsewhere.²⁰ The illumination was only used during the growth of the p-GaN layer to avoid unintentional effects during the cooldown, such as the post-growth annealing.²⁶ Further details on changes in the illumination power and the requirement of above bandgap energy are found elsewhere.²⁷

SIMS analysis was obtained using a CAMECA IMS-6f with a magnetic sector analyzer. The error for all SIMS analyses is 20% after calibration was done against an ion-implanted standard for each species of interest. Analysis for H was achieved using a Cs^+ primary beam and detection of negative secondary ions. The 15 nA primary beam was typically rastered over a $120 \times 120 \mu\text{m}^2$ area with

ions detected from a $30 \mu\text{m}$ diameter region at the center of the raster. The error for the analysis is 20% after calibration was done against an ion-implanted standard. The analysis of Mg was made using an O_2^+ primary beam with 50 nA current rastered over a $180 \times 180 \mu\text{m}^2$ area and positive secondary ions detected from a $60 \mu\text{m}$ diameter area at the center of the raster. The photoluminescence measurements were performed at room temperature and 3 K using a 325 nm (56 mW) HeCd laser. The PL setup consisted of a Janis (SHI-RDK-415D) helium closed-cycle cryostat and a Princeton Instruments (SP2750 0.75 m) spectrometer with an attached PIXIS 2K charged-coupled-device (CCD) camera. Electrical characterization was performed on an Ecopia HMS-5500 AHT55T5 Hall effect measurement system. Room temperature resistivity measurements on the annealed films were performed using the van der Pauw method. Ni/Au contacts (20/40 nm thick, respectively) annealed in atmosphere for 10 min at 650 °C were applied.

III. RESULTS

It is established that the formation energy of a point defect directly affects its concentration in a semiconductor crystal.²⁸ For a charged point defect, the formation energy is a function of the chemical potential and Fermi energy. Modifying the Fermi energy, e.g., by doping, influences the incorporation of other charged point defects. This is expected for the equilibrium or near equilibrium processes, as there is a large excess energy available to be exchanged with the Fermi level. As such, doping during growth promotes the formation of compensating defects (either native, extrinsic, or complexes), further reducing the available number of free carriers and in an extreme case, pinning the Fermi level somewhere within the bandgap away from the band edges. Therefore, it is desirable to find methods by which the Fermi level is controlled during growth such that the formation of compensating point defects is inhibited.

In the present work, a point defect control framework based on a non-equilibrium process is used where excess minority carriers are generated by above bandgap illumination inducing a photo-voltage that changes the quasi Fermi level associated with compensating defects (e.g., H and V_N -complexes) and performs work against their incorporation or generation. Details of the technique are provided elsewhere.^{18–21} In essence, the formation energy of the compensating defects increases in this process, while the main dopant remains unaffected. Furthermore, direct evidence for the role of minority carriers in reducing the defect density has been provided, and other effects related to surface illumination as a probable cause of defect reduction has been ruled out.²⁹

Specifically, the increase in the energy of the formation of hydrogen and nitrogen vacancies, the primary compensators in Mg doped GaN, due to illumination is given by¹⁸

$$\Delta E_{ss}^f(H) = (E_{FH} - E_F), \quad (1)$$
$$\Delta E_{ss}^f(V_N) = (E_{FV_N} - E_F),$$

where E_{FH} and E_{FV_N} are defect quasi Fermi levels of H and V_N , respectively, under illumination and E_F is the Fermi level. The dQFL is dependent on the generated photovoltage energy, $E_p = E_{Fn} - E_{Fp}$ (where E_{Fn} and E_{Fp} are the electron and hole quasi

Fermi levels) and the defect ionization energy (E_{ion}). The net increase in the defect formation energy is then approximately given by¹⁸

$$\Delta E = |E_p| - |E_{ion}| \text{ for } |E_p| > |E_{ion}|. \quad (2)$$

Density functional theory (DFT) calculations²⁷ indicate a shallow H donor ($E_{ion} \sim 0$) and a relatively deep V_N donor in the (+3/+1) transition ($E_{ion} \sim 3$ eV). Hence, the increase in the formation energies of the defects of concern is

$$\begin{aligned} \Delta E_{ss}^f(H) &\sim E_p, \\ \Delta E_{ss}^f(V_N) &\sim E_p - 3 \text{ eV}. \end{aligned} \quad (3)$$

In general, above bandgap illumination is predicted to reduce only compensating defects and, in particular, for Mg:GaN reduce shallow H more effectively than self-compensation by the nitrogen vacancy.

To understand the effect of above bandgap illumination on H during growth, SIMS atomic concentration depth profiles of Mg and H were acquired on the Mg:GaN ladder structures grown with and without UV-illumination. It should be noted that undoped and n-type samples with these growth conditions typically have a H concentration in the mid- 10^{17} cm^{-3} and are invariant to the UV-illumination (not presented). With the introduction of Mg into the layers, however, the total H increases. The data presented for Mg and H are above the detection limits for their respective analyses, 1×10^{16} and $1 \times 10^{17} \text{ cm}^{-3}$, and are, therefore, considered the real concentrations within the layers. Figure 1 displays the results for these structures acquired immediately after the growth without any thermal activation anneal. The illustrated portion of the Mg:GaN depth profile highlights two of the layers with Mg doping concentrations at $3 \times 10^{19} \text{ cm}^{-3}$ and $6 \times 10^{18} \text{ cm}^{-3}$. The sample grown without UV-illumination has an overall high H concentration, suggesting the expected H passivation.⁹ Two different behaviors can be discerned: for Mg levels around $6 \times 10^{18} \text{ cm}^{-3}$, the H

concentration follows closely the Mg concentration, and for higher levels around $2 \times 10^{19} \text{ cm}^{-3}$, the H concentration saturates at a maximum of $\sim 1.5 \times 10^{19} \text{ cm}^{-3}$ as expected from the literature.⁹ On the other hand, for the sample grown under UV-illumination, there is a significant reduction in the overall H concentration for both Mg doping levels. For the lower Mg concentration of $6 \times 10^{18} \text{ cm}^{-3}$, the H level is reduced down to a concentration of $2-3 \times 10^{18} \text{ cm}^{-3}$. Furthermore, for the Mg concentration above $\sim 2 \times 10^{19} \text{ cm}^{-3}$, a reduction in the H level is observed down to a concentration of $8 \times 10^{18} \text{ cm}^{-3}$. It is important to note that the UV-illumination does not influence the Mg concentration, and the observed concentrations agree with what is expected for the used Mg-flow.

Atomic concentrations of O, C, and Si were also measured by SIMS. The actual atomic concentrations of both O and Si could not be determined as they were below their corresponding background levels for the particular measurement: less than $1 \times 10^{18} \text{ cm}^{-3}$ and $1 \times 10^{17} \text{ cm}^{-3}$, respectively. Consequently, O and Si are not considered to be the main compensators in Mg:GaN.³⁰ In addition, the atomic concentration of C was constant at $\sim 1 \times 10^{18} \text{ cm}^{-3}$ independent of UV-illumination.

Our p-type GaN activation conditions provide for a minimum resistivity of around $1.5-3 \Omega\text{cm}$ for Mg concentrations of $2 \times 10^{19} \text{ cm}^{-3}$ and the growth conditions chosen for this experiment. This resistivity is commonly quoted in the literature and is considered to indicate "full" activation.^{5,17,25,31,32} SIMS measurements confirm a reduction of atomic hydrogen by annealing to a concentration of around $2 \times 10^{18} \text{ cm}^{-3}$ for Mg doping levels in the mid- 10^{18} cm^{-3} range. This H concentration agrees with other SIMS measurements after "full" activation by annealing of p-type GaN samples (not shown).

Figure 2 shows SIMS atomic concentration depth profiles for the samples presented in Fig. 1 after an anneal following the previously described conditions. Both samples show comparable levels of hydrogen after annealing. This demonstrates that growth under UV-illumination reduces the amount of hydrogen to a similar

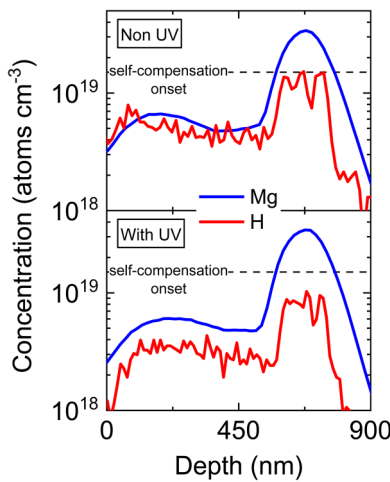


FIG. 1. SIMS on Mg:GaN with and without UV illumination during growth.

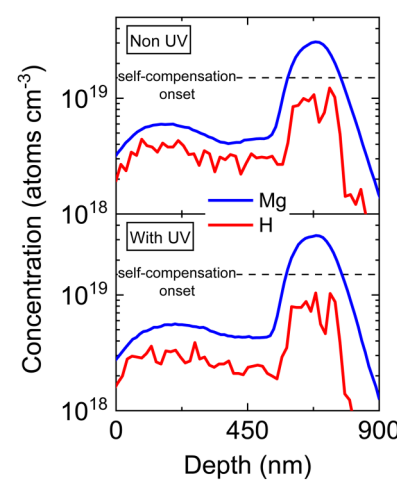


FIG. 2. SIMS on Mg:GaN with and without UV-growth annealed in nitrogen.

TABLE I. Van der Pauw Hall effect of activated Mg:GaN samples grown with and without above bandgap illumination.

	Mg concentration (atoms cm ⁻³)	1 × 10 ¹⁹	2 × 10 ¹⁹	3 × 10 ¹⁹	4 × 10 ¹⁹
Resistivity (Ω cm)	Non-UV	9	1.5	12	36
	With UV	2	1.4	8	11
Hole concentration (×10 ¹⁶ cm ⁻³)	Non-UV	8.4	41	9.4	4.7
	With UV	22	47	10	7.5
Mobility (cm ² V ⁻¹ s ⁻¹)	Non-UV	8.3	11	6.7	3.7
	With UV	14	9.5	7.8	7.6

degree as the post-growth annealing. It is important to note that for a Mg doping level of 2×10^{19} cm⁻³, the sample still has a H concentration of 8×10^{18} cm⁻³ independent of illumination during growth or post-growth annealing. This suggests that this amount of hydrogen is not bound to the Mg in the expected Mg-H configuration at this doping concentration and, therefore, does not respond with further dissociation.⁹ This amount of hydrogen could be present in a different charge state or form a different complex, such as bound to V_N (like the V_N-H complex),^{13,14} making it stable against annealing or illumination during growth.

The boundary between the two H incorporation levels in SIMS could be understood in terms of the self-compensation onset that is also displayed in the resistivity measurements.⁹ Below the onset, H is present at the same concentration as Mg before the activation anneal; thus, H bonding to Mg in the form of Mg-H complexes is expected. Self-compensation by V_N and complexes plays a minor role. Above the self-compensation onset of around 2×10^{19} cm⁻³, not all Mg is bonded to H. Thus, passivation by the Mg-H complex cannot be the main reason for the increase in resistivity. Figure 2 clearly indicates that hydrogen formation in the form of hydrogen donors or complexes becomes less favorable at Mg concentrations above $\sim 2 \times 10^{19}$ cm⁻³, similar to the observation by Castiglia *et al.*⁹ This argument justifies the reasoning that above this limit, native point defect complexes, such as Mg-V_N¹¹ or V_{Ga}(V_{NS}),^{15,16} are involved in the compensation.^{11,15-16} Due to the lower amount of hydrogen, V_N-H compensating complexes can be excluded as the main compensating point defect at this higher doping range.^{13,14}

This discussion puts in perspective the effect of the UV-illumination in the incorporation of H. Overall, there is a significant reduction in the H incorporation when the Mg:GaN is grown under UV-illumination, independent of the Mg concentration and its relation with the self-compensation onset. This indicates that above bandgap illumination suppresses the incorporation of H as a charged defect (H⁺), reducing the formation of the Mg-H complex during growth. It is important to note that illumination only has an effect on defects in a charged state, while having no influence on neutral species. Additionally, the resistivity measurements (Table I) reveal that with proper activation and use of Ni/Au contacts, the UV-grown samples have a slight decrease in resistivity in comparison with non-UV-growth. This suggests that the UV illumination has a further effect on the H incorporation as a compensator and provides a benefit beyond the dissociation of the Mg-H complex by thermal annealing.

To confirm and extend the observations from the SIMS measurements, optical photoluminescence spectra were acquired to

show the impact of UV-illumination on the incorporation of compensating V_N defects and its complexes. As discussed, below the self-compensation onset of 2×10^{19} cm⁻³, the electrical properties of Mg:GaN are dominated by the passivation of Mg by H. Doping above this limit leads to self-compensation dominated by V_N or its complexes, such as Mg-V_N¹¹ or V_{Ga}(V_{NS}),^{15,16} and a corresponding increase in resistivity. PL spectra of UV and non-UV-grown samples were measured for Mg doping concentrations ranging from 1 to 5×10^{19} cm⁻³. The samples were measured both before and after the post-growth annealing procedure. However, the typical donor acceptor pair (DAP) peak at 3.27 eV for Mg doping below 2×10^{19} cm⁻³ appeared only after the anneal. For the samples with doping above this concentration, PL spectra do not show a difference before and after annealing. For consistency, only the spectra acquired after the annealing procedure will be presented.

In Fig. 3, two broad defect transitions can be observed for Mg:GaN at room temperature (RT): the yellow luminescence centered at 2.2 eV and the blue luminescence centered at 2.8 eV. The origin of the yellow luminescence is still controversial, but it has been attributed to V_{Ga},³³ C_N,³⁴ or C-related complexes such as C_N-O_N.³⁵ It is present in all samples, and no significant changes can be observed as a function of doping or UV illumination. The observation of a constant 1×10^{18} cm⁻³ C concentration measured with SIMS for all samples supports the connection to the 2.2 eV luminescence. Since UV illumination is supposed to reduce compensation by unintentional donors in p-type GaN, and the C remained invariant, this observation supports the general interpretation of the yellow luminescence being connected to C_N³⁴ or the C_N-O_N defect complex in GaN.³⁵

However, the impact of the UV illumination on the blue luminescence at 2.8 eV is significant. As shown in Fig. 3, the 2.8 eV donor acceptor pair (DAP) luminescence appears at Mg doping concentrations above the self-compensation onset at 2×10^{19} cm⁻³.³⁶ The origin of the blue luminescence has been related to a V_N-Mg donor and Mg acceptor DAP transition,³⁷ but more recent studies have shown a relationship to V_{Ga}(V_N)₂ or V_{Ga}(V_N).^{15,16} The observation of the 2.8 eV luminescence is, therefore, an indication for the onset of self-compensation in Mg:GaN. All samples grown under UV illumination with Mg concentration above 2×10^{19} cm⁻³ demonstrate a decrease in the blue luminescence at 2.8 eV, indicating a reduction in self-compensation of Mg.

Similarly, the low temperature photoluminescence spectra display clear evidence of compensation reduction using dQFL control. In Fig. 4, the spectra acquired at 3 K for the samples presented in Fig. 3 are shown. Now, the prominent DAP transition at

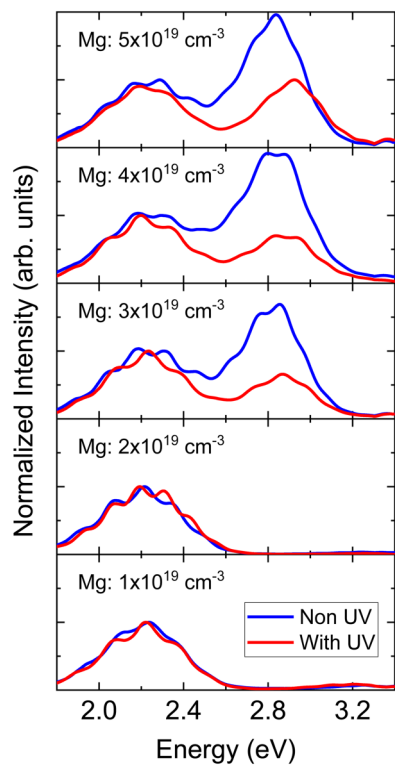


FIG. 3. RT PL luminescence of samples grown with and without UV illumination.

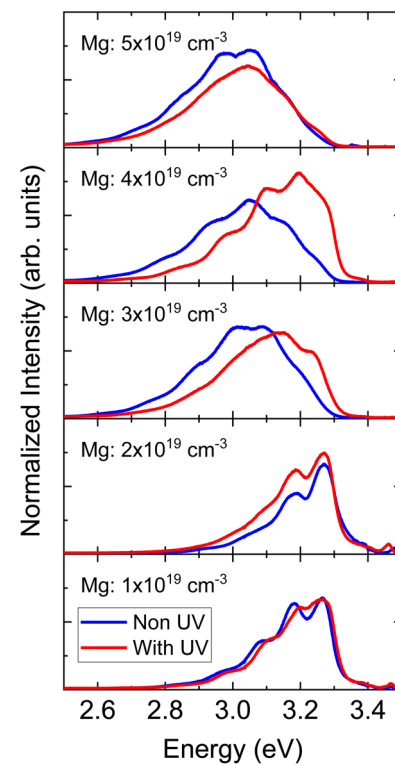


FIG. 4. 3K PL luminescence of samples grown with and without UV illumination.

3.27 eV related to Mg acceptors is observed in the spectra.³⁷ Typically, this peak is expected for Mg concentrations before the onset of nitrogen vacancy related self-compensation. In addition, acceptor bound exciton transitions can be observed if the Mg has been activated by post-growth annealing (3.4–3.5 eV).³⁸ Indeed, the non-illuminated samples show this transition from Mg acceptor DAP at 3.27 eV to the nitrogen vacancy related “blue” compensation peak at ~2.8 eV once the Mg concentration exceeds $2 \times 10^{19} \text{ cm}^{-3}$.¹⁶ At an intermediate stage, one can see an overlap of these transitions leading to a maximum PL at ~3 eV. However, the use of UV illumination delays this transition to the luminescence at 2.8 eV. Illuminated samples with Mg concentrations of $3\text{--}4 \times 10^{19} \text{ cm}^{-3}$ do not have the strong emission at 2.8 eV and maintain the acceptor related transition at 3.27 eV. At the highest Mg doping level, the self-compensation related peak at ~2.8 eV dominates both spectra, but the UV-illumination reduces the intensity of this peak. Thus, the PL results for room temperature and 3 K indicate a reduction in self-compensation of Mg when the dQFL control process is adopted.

Data presented thus far provide the compelling evidence that above bandgap illumination reduces both the H and V_N -related defects that incorporate during a Mg:GaN growth. The samples were further studied using van der Pauw Hall effect measurements to assess the impact on the electrical properties and confirm the

reduction in passivation and compensation from the SIMS and PL data above. Initially, the samples were tested as-grown with soldered In for contacts to avoid any potential “activation” by the post-contact deposition anneal required by the traditional Ni/Au stack. The non-UV grown samples were too resistive for measurement as expected from the literature.^{6–9} However, resistivity of the UV-grown samples was measured, and values of 11, 3, and $16 \Omega\text{cm}$ were obtained for Mg concentrations of 1, 2, and $3 \times 10^{19} \text{ cm}^{-3}$, respectively. These values are higher than the samples measured with the Ni/Au contacts and treated with the post-growth thermal activation (Table I), but it is not clear if this is due to poor ohmic contact formation with soldered In or if the samples were not fully “activated” by skipping the annealing step. Despite this limitation, the results are still remarkable because they indicate some of the Mg atoms are entering the film as acceptor dopants via this dQFL control process and not in the neutral Mg–H complex.^{6–9}

Table I lists the resistivity, free hole concentration, and mobility for the samples with Mg concentrations ranging from 1 up to $4 \times 10^{19} \text{ cm}^{-3}$ after post-growth thermal activation, and Ni/Au p-type contacts were deposited. The highest doped samples of $5 \times 10^{19} \text{ cm}^{-3}$ were too resistive to achieve an ohmic contact needed for Hall measurements³⁹ and have been excluded from the discussion. Two main regions of increased resistivity were observed centered around a Mg doping concentration of $\sim 2 \times 10^{19} \text{ cm}^{-3}$. As

expected from the literature and our previous results, this concentration represents a typical “minimum” in the resistivity where the H concentration saturates, and the onset of the V_N -related self-compensation begins.

Beginning with the Mg doping level of $1 \times 10^{19} \text{ cm}^{-3}$, the resistivity was reduced from 9 to $2 \Omega\text{cm}$ when the sample was illuminated with above bandgap light. This corresponded to an increase in the free hole concentration by a factor of 2.5 and the mobility by 2.7. The root of the improvement, however, is not immediately evident. Because the V_N -related defect peak was not observed in the PL, and previous work suggests that the $V_{\text{Ga}}(V_N)$ ($s = 2$ or 3) complexes do not increase in concentration until Mg doping exceeds $1 \times 10^{19} \text{ cm}^{-3}$,^{15,16} the V_N -related compensation is not expected to affect the resistivity for this doping level. Instead, it is proposed that the resistivity reduction is due to an illumination effect on the residual H. Although SIMS confirmed the total H concentration after activation was similar between the conventional and dQFL-grown samples (Figs. 1 and 2), it cannot determine the defect configuration of this residual H, i.e., if it is charged, neutral, or exists as a complex. As such, it is proposed that the illumination causes the residual H to incorporate in a more neutral configuration that does not compensate the Mg, similar to the effect of illumination on the C impurity in n-type GaN.²⁷

Above the self-compensation onset, the UV-illuminated samples also demonstrated a clear improvement to the electrical characteristics. At the Mg doping concentration of $3 \times 10^{19} \text{ cm}^{-3}$, the measured resistivity decreased from 12 to $8 \Omega\text{cm}$, with slight increases in the hole concentration and mobility in the Hall measurement. A more pronounced effect was observed for the $4 \times 10^{19} \text{ cm}^{-3}$ Mg doping level, where the resistivity decreased to $11 \Omega\text{cm}$ from $36 \Omega\text{cm}$, and an increase in the free hole concentration by a factor 1.5 and mobility by 2 was observed. Since the H concentration saturates well before these doping levels, the change in resistivity is interpreted as a decrease in the V_N -related compensation. From the PL spectra, the blue luminescence associated with the V_N -complexes is either reduced at room temperature (Fig. 3) or shifted back to the DAP at low temperature (Fig. 4). In the previous work,^{15,16} the appearance of the blue luminescence peak at a Mg concentration greater than $1 \times 10^{19} \text{ cm}^{-3}$ was correlated to an increased $V_{\text{Ga}}(V_N)$ ($s = 2$ or 3) concentration. From the diminished blue luminescence signals in Figs. 3 and 4, it is concluded that the UV-illumination reduced the incorporation of these V_N -complexes and led to the improved resistivity of the films.

In general, the UV-grown samples showed a lower resistivity with higher free hole concentrations and mobilities than the annealed, non-UV-grown samples. This supports the conclusion that the above bandgap illumination reduced both H passivation and V_N -related self-compensation. It should be noted that the V_N formation depends strongly also on the process supersaturation, which was not a part of this study, and can be further reduced from the levels reported herein.

IV. CONCLUSIONS

A defect quasi-Fermi level point defect control process was used to control compensation in Mg doped GaN. For Mg concentrations at or below the self-compensation onset of $\sim 2 \times 10^{19} \text{ cm}^{-3}$,

the use of above bandgap illumination by UV-light during growth reduces the amount of H to similar concentrations as achieved in the standard post-growth annealing process. For Mg concentrations above the self-compensation onset, photoluminescence measurements reveal a significant reduction in the blue luminescence associated with V_N and its complexes. Corresponding electrical measurements reveal that samples grown with above bandgap illumination resulted in lower resistivity values than samples grown without the UV-light, and confirm the reduction in compensation using this dQFL control process. These experimental results are in quantitative agreement with the theoretical framework of point defect control via generation of minority carriers in a steady state above bandgap illumination process. This process is based on the following general rules: (1) the illumination significantly affects the minority carriers (not majority carries); (2) the change in the minority carrier concentration impacts the formation energy of compensating defects, which in turn reduces their concentration; and (3) the applied UV-illumination does not influence the growth itself, i.e., temperature, pre-reactions, or surface kinetics.

ACKNOWLEDGMENTS

The authors gratefully acknowledge partial financial support from National Science Foundation (NSF) (Nos. ECCS-1508854, ECCS-1610992, DMR-1508191, and ECCS-1653383), Army Research Office (ARO) (Nos. W911NF-04-D-0003, W911NF-15-2-0068, and W911NF-16-C-0101), Air Force Office of Scientific Research (AFOSR) (No. FA9550-17-1-0225), Department of Energy (DOE) (No. DE-SC0011883), and ARPA-E (No. DE-AR0000299). Part of this research was performed while one of the authors (M. P. Hoffmann) held a National Research Council Research Associateship. Part of this work was performed at the Analytical Instrumentation Facility (AIF) at North Carolina State University, which is supported by the State of North Carolina and the National Science Foundation (Award No. ECCS-1542015). The AIF is a member of the North Carolina Research Triangle Nanotechnology Network (RTNN), a site in the National Nanotechnology Coordinated Infrastructure (NNCI). The authors thank Fred Stevie and his co-workers at the AIF for their contribution to the SIMS analysis.

REFERENCES

- ¹H. Amano, M. Kito, K. Hiramatsu, and I. Akasaki, *Jpn. J. Appl. Phys.* **28**, L2112 (1989).
- ²I. Akasaki, H. Amano, M. Kito, and K. Hiramatsu, *J. Lumin.* **48–49**, 666 (1991).
- ³S. Nakamura, M. Senoh, S. Nagahama, N. Iwasa, T. Yamada, T. Matsushita, H. Kiyoku, and Y. Sugimoto, *Jpn. J. Appl. Phys.* **35**, L74 (1996).
- ⁴M. Kneissl, T. Kolbe, C. Chua, V. Kueller, N. Lobo, J. Stellmach, A. Knauer, H. Rodriguez, S. Einfeldt, Z. Yang, N. M. Johnson, and M. Weyers, *Semicond. Sci. Technol.* **26**, 014036 (2011).
- ⁵W. Götz, N. M. Johnson, J. Walker, D. P. Bour, and R. A. Street, *Appl. Phys. Lett.* **68**, 667 (1996).
- ⁶W. Götz, N. M. Johnson, J. Walker, D. P. Bour, M. D. McCluskey, and E. E. Haller, *Appl. Phys. Lett.* **69**, 3725 (1996).
- ⁷S. Nakamura, T. Mukai, M. Senoh, and N. Iwasa, *Jpn. J. Appl. Phys.* **31**, L139 (1992).
- ⁸Y. Nakano, O. Fujishima, and T. Kachi, *J. Appl. Phys.* **96**, 415 (2004).
- ⁹A. Castiglia, J. F. Carlin, and N. Grandjean, *Appl. Phys. Lett.* **98**, 213505 (2011).

¹⁰H. Obloh, K. H. Bachem, U. Kaufmann, M. Kunzer, M. Maier, A. Ramakrishnan, and P. Schlotter, *J. Cryst. Growth* **195**, 270 (1998).

¹¹U. Kaufmann, P. Schlotter, H. Obloh, K. Köhler, and M. Maier, *Phys. Rev. B* **62**, 10867 (2000).

¹²R. Kirste, M. P. Hoffmann, J. Tweedie, Z. Bryan, G. Callsen, T. Kure, C. Nenstiel, M. R. Wagner, R. Collazo, A. Hoffmann, and Z. Sitar, *J. Appl. Phys.* **113**, 103504 (2013).

¹³F. Shahedipour and B. W. Wessels, *Appl. Phys. Lett.* **76**, 3011 (2000).

¹⁴O. Gelhausen, M. R. Phillips, E. M. Goldys, T. Paskova, B. Monemar, M. Strassburg, and A. Hoffmann, *Phys. Rev. B* **69**, 125210 (2004).

¹⁵A. Uedono, S. Takashima, M. Edo, K. Ueno, H. Matsuyama, H. Kudo, H. Naramoto, and S. Ishibashi, *Phys. Status Solidi B* **252**(12), 2794 (2015).

¹⁶S. F. Chichibu, K. Shima, K. Kojima, S. Takashima, M. Edo, K. Ueno, S. Ishibashi, and A. Uedono, *Appl. Phys. Lett.* **112**, 211901 (2018).

¹⁷B. Sarkar, S. Mita, P. Reddy, A. Klump, F. Kaess, J. Tweedie, I. Bryan, Z. Bryan, R. Kirste, E. Kohn, R. Collazo, and Z. Sitar, *Appl. Phys. Lett.* **111**, 032109 (2017).

¹⁸P. Reddy, M. P. Hoffmann, F. Kaess, Z. Bryan, I. Bryan, M. Bobea, A. Klump, J. Tweedie, R. Kirste, S. Mita, M. Gerhold, R. Collazo, and Z. Sitar, *J. Appl. Phys.* **120**, 185704 (2016).

¹⁹M. P. Hoffmann, J. Tweedie, R. Kirste, Z. Bryan, I. Bryan, M. Gerhold, Z. Sitar, and R. Collazo, *Proc. SPIE* **8986**, 89860T (2014).

²⁰Z. Bryan, M. Hoffmann, J. Tweedie, R. Kirste, G. Callsen, I. Bryan, A. Rice, M. Bobea, S. Mita, J. Xie, Z. Sitar, and R. Collazo, *J. Electron. Mater.* **42**, 815 (2012).

²¹Z. Bryan, I. Bryan, B. E. Gaddy, P. Reddy, L. Hussey, M. Bobea, W. Guo, M. Hoffmann, R. Kirste, J. Tweedie, M. Gerhold, D. L. Irving, Z. Sitar, and R. Collazo, *Appl. Phys. Lett.* **105**, 222101 (2014).

²²C. E. Sanders, D. A. Beaton, R. C. Reedy, and K. Alberi, *Appl. Phys. Lett.* **106**, 182105 (2015).

²³R. Kirste, M. P. Hoffmann, E. Sachet, M. Bobea, Z. Bryan, I. Bryan, C. Nenstiel, A. Hoffmann, J.-P. Maria, R. Collazo, and Z. Sitar, *Appl. Phys. Lett.* **103**, 242107 (2013).

²⁴S. Mita, R. Collazo, A. Rice, J. Tweedie, J. Q. Xie, R. Dalmau, and Z. Sitar, *Phys. Status Solidi C* **8**(7–8), 2078–2080 (2011).

²⁵Y. Kamiura, Y. Yamashita, and S. Nakamura, *Physica B Condens. Matter* **273–274**, 54 (1999).

²⁶Y. Kamiura, Y. Yamashita, and S. Nakamura, *Jpn. J. Appl. Phys.* **37**, L970 (1998).

²⁷F. Kaess, P. Reddy, D. Alden, A. Klump, L. H. Hernandez-Balderrama, A. Franke, R. Kirste, A. Hoffmann, R. Collazo, and Z. Sitar, *J. Appl. Phys.* **120**, 235705 (2016).

²⁸C. G. Van de Walle and J. Neugebauer, *J. Appl. Phys.* **95**, 3851 (2004).

²⁹P. Reddy, F. Kaess, J. Tweedie, R. Kirste, S. Mita, R. Collazo, and Z. Sitar, *Appl. Phys. Lett.* **111**, 152101 (2017).

³⁰Z. Liliental-Weber, J. Jasinski, M. Benamara, I. Grzegory, S. Porowski, D. J. H. Lampert, C. J. Eiting, and R. D. Dupuis, *Phys. Status Solidi B Basic Res.* **228**, 345 (2001).

³¹B. Fu, N. Liu, N. Zhang, Z. Si, X. Wei, X. Wang, H. Lu, Z. Liu, T. Wei, X. Yi, J. Li, and J. Wang, *J. Electron. Mater.* **11**, 1 (2014).

³²Y. Nakagawa, M. Haraguchi, M. Fukui, S. Tanaka, A. Sakaki, K. Kususe, N. Hosokawa, T. Takehara, Y. Morioka, H. Iijima, M. Kubota, M. Abe, T. Mukai, H. Takagi, and G. Shinomiya, *Jpn. J. Appl. Phys.* **43**, 23 (2004).

³³J. Neugebauer and C. G. Van de Walle, *Appl. Phys. Lett.* **69**, 503 (1996).

³⁴J. L. Lyons, A. Janotti, and C. G. Van de Walle, *Appl. Phys. Lett.* **97**, 152108 (2010).

³⁵D. O. Demchenko, I. C. Diallo, and M. A. Reschikov, *Phys. Rev. Lett.* **110**, 087404 (2013).

³⁶M. A. Reschikov, G. C. Yi, and B. W. Wessels, *Phys. Rev. B* **59**, 13176 (1999).

³⁷U. Kaufmann, M. Kunzer, M. Maier, H. Obloh, A. Ramakrishnan, B. Santic, and P. Schlotter, *Appl. Phys. Lett.* **72**, 1326 (1998).

³⁸G. Callsen, M. R. Wagner, T. Kure, J. S. Reparaz, M. Bügler, J. Brunnmeier, C. Nenstiel, A. Hoffmann, M. Hoffmann, J. Tweedie, Z. Bryan, S. Aygun, R. Kirste, R. Collazo, and Z. Sitar, *Phys. Rev. B* **86**, 075207 (2012).

³⁹B. Sarkar, P. Reddy, A. Klump, F. Kaess, R. Rounds, R. Kirste, S. Mita, E. Kohn, R. Collazo, and Z. Sitar, *J. Electron. Mater.* **47**(1), 305 (2018).